Front. Optoelectron. 2013, 6(2): 134–145
DOI 10.1007/s12200-013-0319-9

REVIEW ARTICLE

Recent advances of optical imaging in animal stroke model

Zhen WANG (✉)[1,2]

1 Britton Chance Center for Biomedical Photonics, Wuhan National Laboratory for Optoelectronics, Huazhong University of Science and Technology, Wuhan 430074, China
2 MoE Key Laboratory for Biomedical Photonics, Department of Biomedical Engineering, Huazhong University of Science and Technology, Wuhan 430074, China

Abstract Stroke is a major health concern and an intensive research subject due that it is the major cause of death and the leading cause of disability worldwide. The past three decades of clinical disappointments in treating stroke must compel us to rethink our strategy. New effective protocol for stroke could greatly benefit from the advances in optical imaging technologies. This review focuses on the latest advance of applications of three optical imaging techniques in animal model of stroke, such as photoacoustic (PA) imaging, laser speckle contrast imaging (LSCI) and two-photon microscopy (TPM). The potential roles of those techniques in the future of stroke management are also discussed.

Keywords optical imaging, photoacoustic (PA) imaging, laser speckle contrast imaging (LSCI), two-photon microscopy (TPM), animal model, stroke

1 Introduction

Stroke, or cerebrovascular accident, is the rapid loss of brain function due to disturbance in the blood supply to the brain. This can be due to ischemia caused by blockage, or hemorrhage [1]. Stroke is the major cause of death and the leading cause of disability worldwide. It is projected that between the years of 2005–2050 the care of stroke patients will cost an estimated 1.52 trillion dollars [2]. Therefore, stroke is a major health concern and an intensive research subject.

Considerable advances have been made in understanding the pathology of ischemic stroke. Although interrupting key pathogenic mechanisms has significantly improved outcome in animal stroke models, translating those into effective clinical treatments has been challenging [3]. The past three decades of clinical disappointments in treating stroke must compel us to rethink our strategy [3].

Current high resolution brain imaging methods in clinic include X-ray computed tomography (CT), magnetic resonance imaging (MRI), and ultrasound. However, CT uses ionizing radiation and MRI uses a strong magnetic field, and both methods are costly. Ultrasonography can only be used in pediatric brain imaging, and then only before closure of the fontanel. In addition, functional brain images are provided by functional MRI (fMRI), electroencephalography (EEG), magnetoencephalography (MEG), positron emission tomography (PET), single photon emission computed tomography (SPECT). Only fMRI, PET and SPECT can provide high resolution. But fMRI is expensive and has a low temporal resolution, and PET and SPECT use radioactive contrast agents [4].

Compared to MRI, optical technology promises to be quicker, cheaper, simpler, and more versatile [3]. New effective protocol for stroke could greatly benefit from the advances in optical technologies.

The use of novel optical imaging technologies has been instrumental for a number of central discoveries in both basic and clinical neuroscience, and Fig. 1 shows an overview of optical imaging technologies with different resolutions and penetration depth [5]. Optical imaging tools have played an important role in the study of neurovascular and neurometabolic disregulation in animal models of stroke [6]. Likewise, noninvasive optical technologies have started making inroads into bedside imaging of blood flow and oxygen consumption in human stroke patients [7,8].

This review mainly focuses on the latest advance of applications of three optical imaging techniques in animal model of stroke, such as photoacoustic (PA) imaging, laser speckle contrast imaging (LSCI) and two-photon microscopy (TPM). The potential roles of those optical imaging techniques in the future of stroke management are also discussed.

Received January 30, 2013; accepted February 21, 2013

E-mail: zhenwang@mail.hust.edu.cn

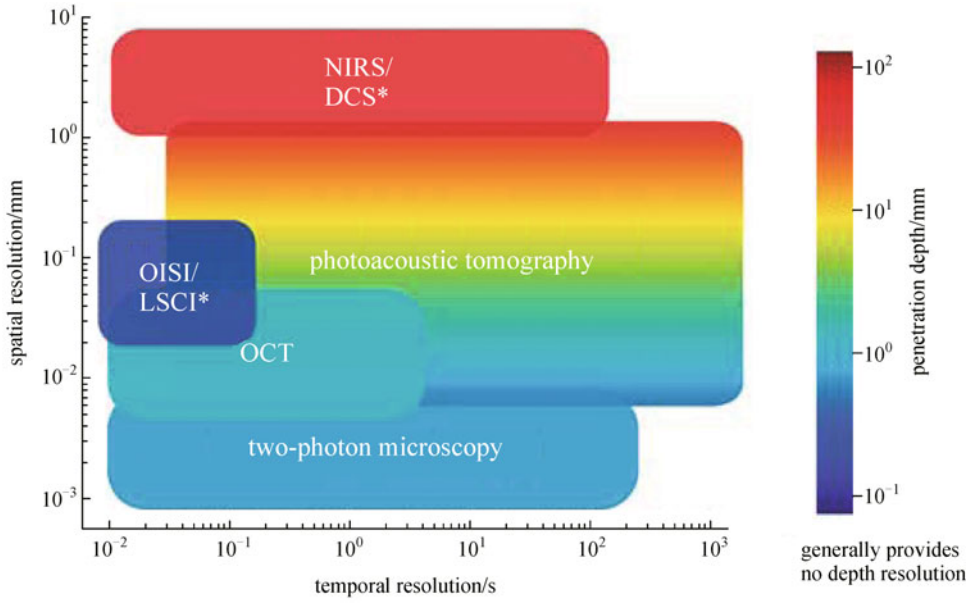

Fig. 1 Comparison of spatial resolution, temporal resolution, and penetration depth among optical imaging techniques. Plot of the spatial and temporal resolutions of different optical techniques, with color-coded penetration depth is presented. Near-infrared spectroscopy (NIRS); diffuse correlation spectroscopy (DCS); optical intrinsic signal imaging (OISI); laser speckle contrast imaging (LSCI) and optical coherence tomography (OCT). This figure was reprinted from Ref. [5]

2 Parameters accessible to optical imaging measurements

Before we start our review of the studies, we will provide a brief overview of the parameters accessible to optical imaging measurements in stroke [9].

2.1 Changes in hemoglobin concentrations

Changes in the concentrations of oxygenated hemoglobin (HbO), deoxygenated hemoglobin (HbR) and their sum, total hemoglobin (HbT), where HbT = HbO + HbR, have been able to be determined in stroke. But absolute quantification of HbO and HbR is not yet reliable enough to allow the definition of thresholds for ischemia [9].

2.2 Blood and tissue oxygenation

There have been several attempts to define a parameter that avoids the issue of absolute quantification of HbR and HbO, but still supplies a value that can be used as a threshold to monitor the brain potentially in acute stroke care [9]. Such values usually target cerebral blood or tissue oxygenation (rSO2: regional oxygen saturation; TOI: tissue oxygenation index). The terms blood and tissue oxygenation are used interchangeably in the literature [9].

2.3 Cerebral perfusion and blood flow

Since stroke is caused by a reduction of cerebral blood flow (CBF), the ability of optical imaging to monitor cerebral perfusion has been a focus of research on the changes of blood flow.

2.4 Changes of neuronal structure following stroke

The rapid loss of brain function results from changes of neuronal structure following stroke induced by disturbance in the blood supply to the brain. Changes of neuronal fine structure can be traced by optical imaging tools.

3 Photoacoustic imaging

Since being discovered by Alexander Bell, photoacoustics may be seeing major resurgence in biomedical imaging [10]. It has been broadly studied in biomedicine, for both human and small animal tissues [4]. The fundamental principle of the PA effect can be simply described: An object absorbs electromagnetic radiation energy, the absorbed energy converts into heat, and the temperature of the object increases. As soon as the temperature increases, thermal expansion takes place, generating acoustic pressure in the medium. However, steady thermal expansion (time invariant heating) does not generate acoustic waves; thus, the heating source is required to be time-variant [4]. Although most high-resolution pure optical detection methods are capable of detecting optical absorption, they are generally much less sensitive to optical absorption than PA detection [11].

A primary PA application in biomedicine is photoacoustic tomography (PAT). It is the cross-sectional or three-dimensional (3D) imaging of a material using the photoacoustic effect [12]. Commercially available high-resolution 3D optical imaging modalities — including confocal microscopy, TPM, and optical coherence tomography — have fundamentally impacted biomedicine. Unfortunately, such tools cannot penetrate biologic tissue deeper than the optical transport mean free path ~1 mm in the skin. PAT, which combines strong optical contrast and high ultrasonic resolution in a single modality, has broken through this fundamental depth limitation and achieved superdepth high-resolution optical imaging [13].

Currently, PAT has three major implementations: focused-scanning photoacoustic microscopy (PAM), photoacoustic computed tomography (PACT), and photoacoustic endoscopy (PAE). Whereas, PAM and PAE usually aim to image millimeters deep at micrometerscale resolution, PACT can be implemented for both microscopic and macroscopic imaging [4].

3.1 Photoacoustic imaging and stroke

Optical-resolution PAM (OR-PAM) has been validated as a valuable tool for label-free volumetric microvascular imaging. As we known, a major obstacle in understanding the mechanism of ischemic stroke is the lack of a tool to noninvasively or minimally invasively monitor cerebral hemodynamics longitudinally. Hu et al. in 2011 applied OR-PAM to longitudinally study ischemic stroke induced brain injury in a mouse model with transient middle cerebral artery occlusion (tMCAO) [14]. OR-PAM showed that, during MCAO, the average hemoglobin SO2 values of feeder arteries and draining veins within the stroke core region dropped ~10% and ~34%, respectively. After reperfusion, arterial SO2 recovered back to the baseline; however, the venous SO2 increased above the baseline value by ~7%. Thereafter, venous sO2 values were close to the arterial SO2 values, suggesting eventual brain tissue infarction [14].

Besides, studying cerebral metabolism during ischemia has been limited by imaging modalities that have either good tissue penetration but low spatial resolution, or high resolution requiring invasive preparations (open-skull windows). In 2012, OR-PAM was also employed to longitudinally monitor cerebral metabolism through the intact skull of Swiss Webster mice before, during, and up to 72 h after a 1-h tMCAO (see Fig. 2) [15].

Recently, PAM combined with LSCI has been used to examine the changes in CBF, cerebral blood volume (CBV), and SO2 during and after 3-h acute focal ischemic rats [16]. The study suggested that combining LSCI and PAM provides an attractive approach for stroke detection in small animal studies.

3.2 Limitations of photoacoustic imaging and outlook

PAT has limitations, as does any imaging technology. First, optical attenuation limits the penetration to ~5 cm when a resolution of less than 1 mm is desired in tissue [17–19]. Microwaves or radio waves can be used for deeper excitation, although the contrast origins differ. Second, ultrasound sustains strong reflection from gas–liquid or gas–solid interfaces, owing to the strong mismatch of acoustic impedances. Therefore, ultrasound signals cannot penetrate through gas cavities or lung tissues efficiently. For the same reason, ultrasonic detection requires direct contact between the ultrasonic transducers and the biologic tissue. Usually, ultrasound coupling gel is applied to the tissue surface to remove intervening air cavities. The development of non-contact optical detection for acoustic displacement is a potential solution to this problem [20–23]. Third, ultrasound suffers from significant attenuation and phase distortion in thick bones, such as the human skull. Fortunately, unlike pulse-echo ultrasound imaging, PAT involves only oneway ultrasound attenuation through the skull. Sufficiently strong photoacoustic signals have been observed through Rhesus monkey skulls [24,25]. The remaining challenge is to compensate for the phase distortion introduced by the skull.

In summary, PAT perfectly complements other biomedical imaging modalities by providing unique optical absorption contrast with highly scalable spatial resolution, penetration depth, and imaging speed. In light of its capabilities and flexibilities, PAT is expected to play a more essential role in stroke studies and clinical practice [26].

4 Laser speckle contrast imaging

4.1 Laser speckle imaging physics

When an object is illuminated with coherent laser light, a speckle pattern, or random interference pattern, is produced at the camera due to the fact that the laser light reaching each pixel has traveled slightly different path lengths and adds coherence, both constructively and destructively. In many imaging systems, speckle is a significant source of noise, and considerable effort has been spent in eliminating speckle. However, the dynamics of the speckle pattern contains information about the motion of the scattering particles in the sample. When some of the scattering particles are in motion (i.e., blood cells), the speckle pattern fluctuates in time. When the exposure time of the camera is longer than the time scale of the speckle intensity fluctuations (typically less than 1 ms for biologic tissues), the camera integrates the intensity variations resulting in blurring of the speckle pattern [27]. In areas of increased motion, there is more blurring of the speckles during the camera exposure resulting in a lower spatial contrast of the speckles in these areas [27].

LSCI has emerged over the past decade as a powerful, yet simple, method for imaging of blood flow dynamics in real time [27]. The rapid adoption of LSCI for physiologic

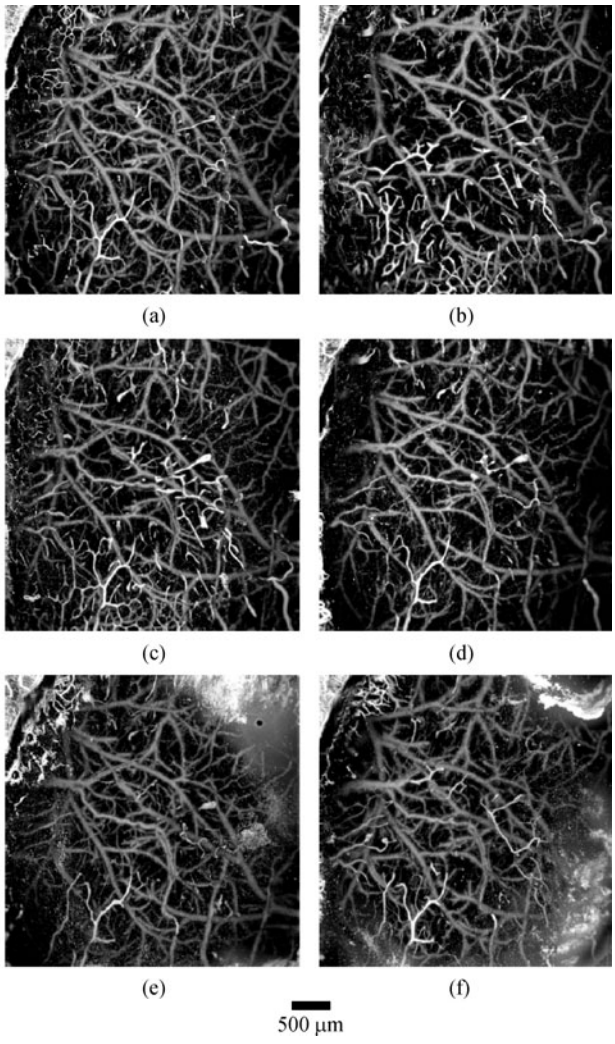

Fig. 2 Longitudinal monitoring of ischemic stroke induced by transient middle cerebral artery occlusion (tMCAO) in the left parietal cortex. (a) Before tMCAO; (b) during tMCAO; (c) after tMCAO; (d) day 3; (e) day 7; (f) day 25. This figure was reprinted from Ref. [15]

studies is due to the relative ease and low cost of building an instrument as well as the ability to quantify blood flow changes with excellent spatial and temporal resolution [27]. Although measurements are limited to superficial tissues with no depth resolution, LSCI has been instrumental in pre-clinical studies of neurological disorders [27]. Recently a number of technical advances have been developed to improve technique, such as the quantitative accuracy, temporal resolution [27], and so on. Those advances were briefly reviewed as follows:

4.1.1 The latest reports on effect of signal intensity and camera quantization on laser speckle contrast analysis was given by Song and Elson in 2013 [28]

As we known, laser speckle contrast analysis (LASCA) is limited to being a qualitative method for the measurement of blood flow and tissue perfusion as it is sensitive to the measurement configuration. The signal intensity is one of the parameters that can affect the contrast values due to the quantization of the signals by the camera and analog-to-digital converter (ADC). In 2013, Song and Elson deduced the theoretical relationship between signal intensity and contrast values based on the probability density function (PDF) of the speckle pattern and simplify it to a rational function [28]. A simple method to correct this contrast error is also suggested [28]. The experimental results demonstrate that this relationship can effectively compensate the bias in contrast values induced by the quantized signal intensity and correct for bias induced by signal intensity variations across the field of view [28].

4.1.2 He et al. presented a lateral laser speckle contrast analysis combined with line beam scanning illumination to improve the sampling depth of blood flow imaging [29]

He et al. presented a lateral laser speckle contrast analysis method combined with line beam scanning illumination to

improve the sampling depth of blood flow imaging [29]. Both the phantom and animal experimental results suggest that localized illumination and LSCA can significantly enhance the deep blood flow signal to improve the sampling depth of LSCI compared with the traditional full-field illumination LSCA method [29].

4.1.3 Furthermore, correcting the detrimental effects of nonuniform intensity distribution on fiber-transmitting laser speckle imaging of blood flow was also presented by Zhang et al. [30]

Laser speckle spatial contrast analysis (LSSCA) is superior to laser speckle temporal contrast analysis (LSTCA) in monitoring the fast change in blood flow due to its advantage of high temporal resolution. However, the application of LSSCA, which is based on spatial statistics, may be limited when there is nonuniform intensity distribution, such as fibertransmitting laser speckle imaging. In this study, Zhang et al. presented a normalized laser speckle spatial contrast analysis (nLSSCA) to correct the detrimental effects of nonuniform intensity distribution on the spatial statistics [30]. Through numerical simulation and phantom experiments, it was found that just ten frames of dynamic laser speckle images are sufficient for nLSSCA to achieve effective correction [30]. Furthermore, nLSSCA has higher temporal resolution than LSTCA to respond the change in velocity [30]. LSSCA, LSTCA and nLSSCA are all applied in the fiber-transmitting laser speckle imaging system to analyze the change of CBF during cortical spreading depression (CSD) in rat cortex respectively, and the results suggest that nLSSCA can examine the change of CBF more accurately. For these advantages, nLSSCA could be a potential tool for fiber transmitting/ endoscopic laser speckle imaging [30].

4.1.4 Song and Elson demonstrated a dual wavelength endoscopic laser speckle contrast imaging system for indicating tissue blood flow and oxygenation [31]

This system has a frame rate of 10 Hz and can rapidly monitor changes in blood flow *in vivo*, using the contrast values of the speckle images recorded with 1 ms exposure time [31]. In addition, the mean intensities can record the respiration period and can indicate changes in tissue oxygenation [31]. This system was tested during an occlusion to a human finger and is being applied in endoscopy [31].

4.1.5 Dual-modal (OIS/LSCI) imager of cerebral cortex in freely moving animals was provided by Lua et al. [32]

LSCI and optical intrinsic signals imaging (OISI) have been used for years in the study of CBF and hemodynamic responses to neural activity. So far, most *in vivo* rodent experiments are based on the anesthesia model when the animals are in unconscious and restrained conditions. As we known, the anesthesia has influences on the neural activity have been documented. Lu et al. designed a miniature head-mounted dual-modal imager in freely moving animals that could monitor in real time the coupling of local oxygen consumption and blood perfusion of CBF by integrating different imaging modalities of OIS and LSCI [32]. The system facilitates the study the cortical hemodynamics and neural-hemodynamic coupling in real time in freely moving animals [32].

4.2 Laser speckle contrast imaging and stroke

Animal models of stroke are widely used to investigate the basic pathophysiology of stroke and to evaluate new stroke therapies. A critical aspect of these studies is monitoring of blood flow dynamics in the brain [33]. Laser Doppler flowmetry has been used for many years in such studies and is widely considered to be the gold standard for quantifying blood flow changes in the brain in animal models of stroke [33]. Although MRI and PET have also been used in animal models of stroke, the spatial and temporal resolution of these techniques is usually not sufficient to enable detailed studies of blood flow dynamics [33]. First introduced in the 1980s, LSCI is a powerful tool for full-field imaging of blood flow [33]. It has been used extensively in animal models of stroke because of its ability to provide real time images of the spatial and temporal blood flow dynamics. Here, a brief review on the latest development of LSCI in animal model of stroke was given as below:

4.2.1 Quantitative imaging of ischemic stroke through thinned skull in mice with multi exposure speckle imaging was reported by Parthasarathy et al. in 2010 [34]

LSCI has become a widely used technique to image cerebral blood flow *in vivo*. However, the quantitative accuracy of blood flow changes measured through the thin skull has not been investigated thoroughly. Parthasarathy et al. have recently developed a new multi exposure speckle imaging (MESI) technique to image blood flow while accounting for the effect of scattering from static tissue elements [34]. The MESI technique was used to image the blood flow changes in a mouse cortex following photothrombotic occlusion of middle cerebral artery [34]. The MESI was found to accurately estimate flow changes due to ischemia in mice brains *in vivo* [34]. These estimates of these flow changes were found to be unaffected by scattering from thinned skull [34].

4.2.2 Rapid monitoring of cerebral ischemia dynamics was achieved in 2012 by using laser-based optical imaging of blood oxygenation and flow [35]

Imaging blood flow or oxygenation changes using optical

techniques is useful for monitoring cortical activity in healthy subjects as well as in diseased states. However, in order to gain a better understanding of hemodynamics in conscious, freely moving animals, these techniques must be implemented in a small scale, portable design that is adaptable to a wearable format. Levy et al. have demonstrated a novel system which combines the two techniques of LSCI and intrinsic optical signal imaging simultaneously, using compact laser sources, to monitor induced cortical ischemia in a full field format with high temporal acquisition rates [35]. They further demonstrated the advantages of using combined measurements of speckle contrast and oxygenation to establish absolute flow velocities, as well as to statistically distinguish between veins and arteries [35]. Levy et al. accomplished this system using coherence reduction techniques applied to vertical cavity surface emitting lasers (VCSELs) operating at 680, 795 and 850 nm. This system uses minimal optical components and can easily be adapted into a portable format for continuous monitoring of cortical hemodynamics [35].

4.2.3 Fast synchronized dual-wavelength laser speckle imaging system for monitoring hemodynamic changes in a stroke mouse model was presented by Ruikang K. Wang's group [36]

Qin et al. described a newly developed synchronized dual-wavelength LSCI system, which contains two cameras that are synchronously triggered to acquire data [36]. The system can acquire data at a high spatiotemporal resolution (up to 500 Hz for 1000 × 1000 pixels) [36]. A mouse model of stroke is used to demonstrate the capability for imaging the fast changes (within tens of milliseconds) in oxygenated and deoxygenated hemoglobin concentration, and the relative changes in blood flow in the mouse brain, through an intact cranium [36]. This novel imaging technology will enable the study of fast hemodynamics and metabolic changes in vascular diseases [36].

4.2.4 LSCI was employed to investigate dynamic change of collateral flow varying with distribution of regional blood flow in acute ischemic rat cortex in 2012 (see Fig. 3) [37]

CBF is critical for the maintenance of cerebral function by guaranteed constant oxygen and glucose supply to brain. Collateral channels (CCs) are recruited to provide alternatives to CBF to ischemic regions once the primary vessel is occluded during ischemic stroke. However, the knowledge of the relationship between dynamic evolution of collateral flow and the distribution of regional blood flow remains limited. Laser speckle imaging was used by Wang et al. to assess dynamic changes of CCs and regional blood flow in a rat cortex with permanent MCAO [37]. It was found that CCs immediately provided blood flow to ischemic territories after MCAO. More importantly, there were three kinds of dynamic changes of CCs during acute stroke: persistent CC, impermanent CC, and transient CC, respectively, related to different distributions of regional blood flow [37].

4.3 Prospect and conclusion of laser speckle contrast imaging

LSCI is a powerful method for real-time visualization of blood flow [27]. It is simple instrumentation and low cost that make LSCI readily accessible for many applications ranging from basic physiology to clinical settings [27]. Traditionally, LSCI has been limited to measurements of relative blood flow changes within a single animal [27]. Recent advances such as MESI, however, should enable chronic imaging of blood flow as well as improve the quantitative accuracy of blood flow imaging [27,34]. In addition, speckle imaging combined with other optical

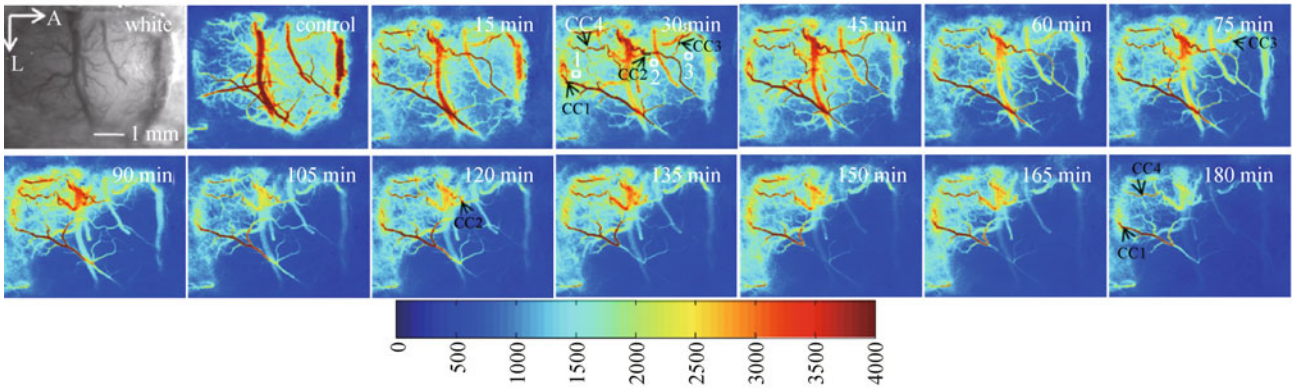

Fig. 3 Spatiotemporal evolution of the distribution of CBF in ischemic cortex by LSCI. After MCAO, the region with low blood perfusion (blue-highlight area) increased with time. And there were dynamic changes in the blood flow of collateral channels (CC). Some of them were persisted (CC1 and CC4); others disappeared with different duration (CC2 and CC3) (A, anterior; L, lateral). This figure was reprinted from Ref. [37]

imaging modalities should enable simultaneous multi-parameter imaging of a range of physiologic parameters [27].

5 Two-photon microscopy

Denk et al. developed the TPM technique, which allows visualizing small structures within the functioning brain of a living organism [38]. By using a pulsed infrared laser that excites fluorophores by the combined power of two long-wavelength photons, it was possible to achieve optical sectioning based on physical principles alone without difficulty in aligning optics or light losses due to confocal pinholes [39]. The use of infrared light was not only necessary for the 2-photon effect, but it had the added advantage of good tissue depth penetration. Optical sectioning result of TPM since the probability of 2-photon excitation is relatively low and is restricted to a narrow focal plane where excitation power is the highest [39].

5.1 Two-photon microscopy and stroke

TPM provides a number of advantages that will aid the study of the mechanisms underlying neurovascular coupling in animal models of stroke [40].

5.1.1 Two-photon microscopy was used to manipulate blood flow with photothrombosis [40]

The majority of current preclinical stroke models focus on large-scale ischemic strokes that manifest severe behavioral deficits [41]. However, small cortical infarcts are prominent in cases of human small vessel disease and dementia, and are clinically difficult to detect [42,43]. Optical access to the vasculature offers the opportunity for laser-mediated formation of intravascular clots in single vessels, as a model to study the effects of small-scale stroke in rats and mice [44–47].

On the cortical surface, single vessel thrombosis is achieved by irradiating the lumen of the target vessel with a focused green laser to activate the circulating photosensitizing dye, Rose Bengal [48,49]. Below the cortical surface, thrombosis is achieved by focusing high-fluence, 100 to 300-fs pulses of near infrared light into the vessel lumen [47]. Nonlinear absorption ensures that the laser injury is limited only to the plane of focus. In this case, damage of the vessel wall induces clot formation in the lumen [47].

Rose Bengal irradiation was applied to occlude one of many penetrating arterioles visible on the pial surface through a dura-removed cranial window in rat (Fig. 4(a)) or a PoRTS window in a CX(3)CR1 transgenic mouse with green fluorescent protein (GFP)-labeled microglia (Fig. 4 (b)).

5.1.2 Longitudinal in situ tracking of transgenic mice with two-photon laser-scanning microscopy can be key method for assessing neuronal structure following all sizes of stroke [40]

By using Thy1-YFP mice, the fine dendritic structure of deep neuronal populations can be imaged over a period of hours to days following stroke [50–52]. In the example of Fig. 5, blood vessels (red channel in Fig. 5(a)) as well as the dendritic arbors of layer 5 neurons (green channel in Fig. 5(a)) are imaged through a dura intact cranial window [53]. Injection of Rose Bengal and irradiation of the vasculature with a broadly focused green laser causes flow to cease in all pial vessels in a region roughly 1 mm^2 in area (right panel in Figs. 5(a) and 5(b)). In this case, severe ischemia leads to rapid dendritic damage over a period of 30 min, as evidenced by blebbing of the dendritic shafts (Figs. 5(c) and 5(d) [54]).

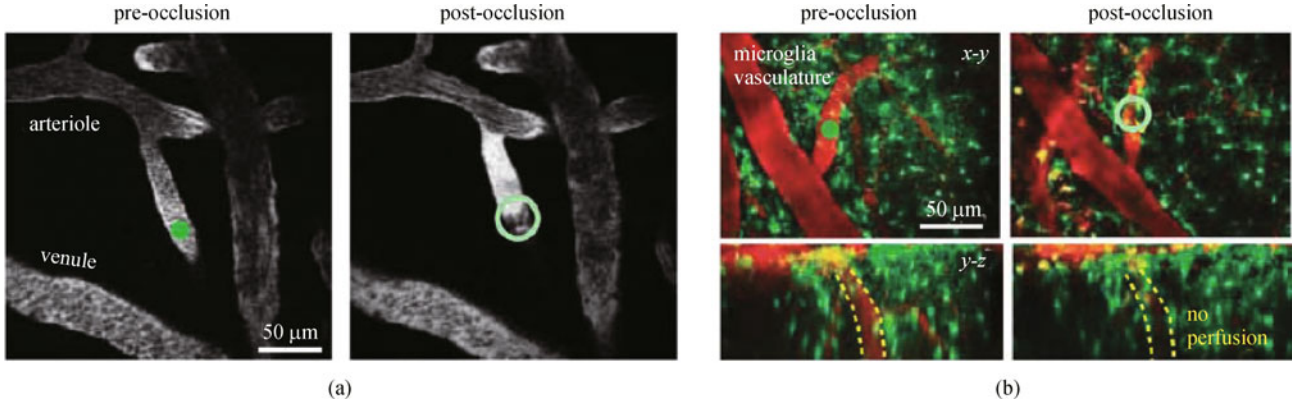

Fig. 4 Manipulation of blood flow in single-cortical vessels using auxiliary lasers. (a) Rose Bengal-mediated photothrombosis of a single penetrating arteriole on the pial surface. Occlusion was achieved after 1 min of irradiation with a green laser focused in the lumen of the target vessel (filled green circle in left panel). The thrombus formed by irradiation sits stably within the lumen surrounded by stagnant serum (open green circle in right panel); (b) photothrombosis of a single mouse penetrating arteriole through a PoRTS window. The CX(3) CR1 mouse line expresses GFP in microglia and monocytes. This figure was reprinted from Ref. [40]

5.1.3 *In vivo* 2-photon imaging has been employed to examine fine structure in the rodent brain before, during, and after stroke [55]

The recent application of TPM to biologic specimens has allowed investigators to examine individual synapses within live animals [55]. In the case of stroke, TPM imaging has revealed marked swelling of dendrites and loss of spines within minutes of ischemic onset [55]. Surprisingly, restoration of blood flow during reperfusion was associated with a return of relatively normal structure [55]. Over longer time scales, TPM imaging revealed elevated rates of synaptogenesis within peri-infarct tissues recovering from stroke [55]. These results provide an example of how high-resolution *in vivo* microscopy can be used to provide insight into both the acute pathology and recovery from stroke damage [55]. It have been outlined how recent advances in TPM have enabled the study of micrometer-level structures such as synapses to be studied in situ (Fig. 6) [55] and to define the vulnerability of the synapse with respect to regional differences in blood flow during stroke and reperfusion (Fig. 6) [55].

5.1.4 Remapping the somatosensory cortex after stroke was reported by Winship and Murphy [60]

Although tissue death occurs within minutes to hours of the onset of reduced blood flow, functional recovery from stroke-induced brain injury continues weeks and months after the initial insult [61]. It has been suggested that this functional recovery occurs via adaptive plasticity in surviving neurons, whereby viable brain tissue reorganizes in order to rebuild or replace damaged synaptic connections and strengthen surviving neuronal networks [61–66]. Indeed, it has been demonstrated in both human stroke patients and animal models of stroke that surviving regions of the cortex can adopt the motor- or sensory-processing functions of regions lost to damage [56,67–70]. *In vivo* 2-photon calcium imaging was introduced to determine how the response properties of individual somatosensory cortex neurons are altered during remapping [60].

5.1.5 Chronic *in vivo* imaging of two-photon microscopy showed no evidence of dendritic plasticity or functional remapping in the contralesional cortex after stroke [71]

Most stroke survivors exhibit a partial recovery from their deficits. This presumably occurs because of remapping of lost capabilities to functionally related brain areas [71]. Functional brain imaging studies suggest that remapping in the contralateral uninjured cortex might represent a transient stage of compensatory plasticity [71]. Some postmortem studies have also shown that stroke can trigger dendritic plasticity in the contralateral hemisphere, but the data are controversial [71]. Longitudinal *in vivo* TPM was used in the contralateral homotopic cortex to record changes in dendritic spines of layer 5 pyramidal neurons in green fluorescent protein mice [71]. Johnston et al. could not detect de novo growth of dendrites or changes in the density or turnover of spines for up to four weeks after stroke [71]. These results suggest that the contralesional cortex may not contribute to functional recovery after stroke and that, at least in mice, the peri-infarct cortex

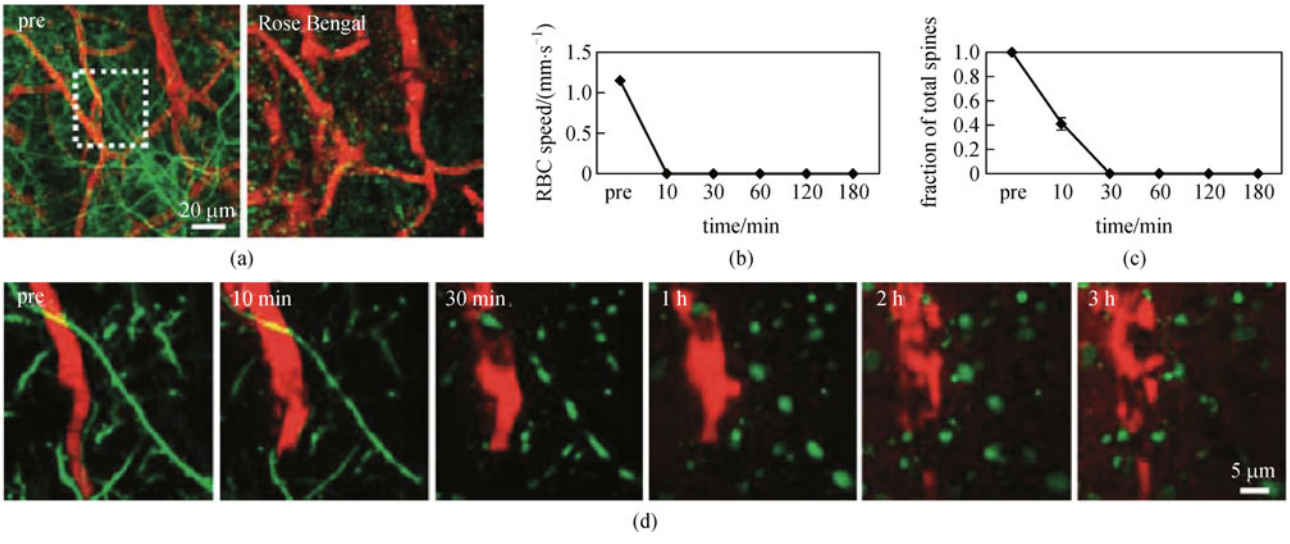

Fig. 5 Imaging of neuronal structure following targeted stroke. (a) Images from a Thy1-YFP mouse showing Texas red-dextranlabeled vasculature (red) and neuronal dendrites (green). The images are maximal intensity projections of the first 100 mm of the cortex before and 30 min after photoactivation of circulating Rose Bengal; (b and c) quantification of red blood cell (RBC) velocity and dendritic spine number for the animal shown in panel a; (d) dendritic structure was completely lost within 30 min of photothrombosis. Residual blood flow after stroke was zero and reperfusion did not occur. Apparent clotting and breakdown of capillaries were seen 30 min after photothrombosis [6]. This figure was reprinted from Ref. [40]

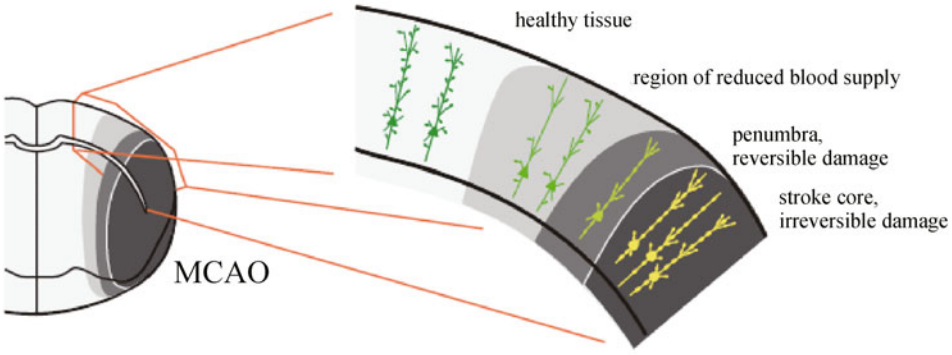

Fig. 6 Relationship between synaptic circuit damage and local blood flow. Cartoon of a cross-section through the rodent cortex showing the stroke core (black) and penumbra (lighter shades of gray) [56] after occlusion of the middle cerebral artery, a common experimental stroke model. The core has < 20% of baseline blood flow and fails to regain its fine dendritic structure after reperfusion [57]. In the penumbra, blood flow increases moving toward the midline as tissues in this region are supplied by other artery systems that were not blocked during the stroke. Within the penumbra, some loss of dendrite structure will reverse when reperfusion occurs and this is where rewiring over longer time scales will occur to replace connectivity lost due to ischemia [57–59]. This figure was reprinted from Ref. [55]

plays the dominant role in postischemic plasticity [71].

5.1.6 Two-photon microscopy has enabled depth-resolved measurements of red blood cell velocities [72] and vascular diameters [73,74]

In the context of blood flow, the TPM technique has enabled depth-resolved measurements of RBC velocities [72] and vascular diameters [73,74] routinely at depths of up to 500 mm deep in the cortex and as deep as 1 mm when utilizing advanced laser systems [75]. In contrast with LSCI, which utilizes Doppler contrast from RBC motion, TPM velocity measurements typically utilize a fluorescent dye to image the blood plasma and track the RBC 'shadows' to estimate velocity in individual capillaries [5]. While LSCI can be generally performed through a thin skull, TPM typically requires a cranial window, although thin skull measurements are now being conducted at the expense of depth penetration [53]. Velocity and diameter measurements are performed on no more than a few vessel segments at a time. As a result, studies that require measurements throughout the vascular geometry to ascertain the collective behavior are not practical with TPM [5].

5.1.7 Combined two-photon microscopy and spectral microCT X-ray imaging to characterize the cellular signature and evolution of microstroke foci [76]

In vivo TPM and transgenic mouse models expressing cell type specific reporters have been used to examine ischemia-related insults, e.g., perturbations of neuronal process morphology and local blood flow in the MCAO [76]. Glia and pericytes can be visualized by selective fluorescent protein expression [76]. In these mice, the breakdown of the blood brain barrier and the immediate as well as long-term cellular responses can be monitored [76].

5.2 Prospect of two-photon microscopy

One major limitation of this method is the need of a fluorescent specimen. Greatly improved staining approaches, however, made it possible to label specific neurons and pathways with genetic tools [77]. We also anticipate that with advances in surgical techniques and further miniaturization of equipment [78,79], such high-resolution measurements will be routinely performed in even awake animals to chart the effects of stroke and recovery. Recent data also suggest that these methods may be important for evaluating the transient effect of peri-infarct depolarization induced by stroke [80].

6 Conclusions

Clinicians' need for real-time information on the structure and function of human systems, as well as effects of disease, such as stroke; optical imaging holds promise in meeting these needs. The great challenge before us is how to make those optical techniques be transferred from bench to bedside. Here are no hard and fast rules but rather a series of lessons from experience. We need to make great efforts to theoretical and technological improvements, so that we can identify when optical imaging will be ready for the patient and what needs to be done to make optical imaging more useful to the patient.

Acknowledgements This work was supported by the Scientific Research Foundation for the Returned Overseas Chinese Scholars, State Education Ministry.

References

1. Sims N R, Muyderman H. Mitochondria, oxidative metabolism and cell death in stroke. Biochimica et Biophysica Acta (BBA)-Molecular Basis of Disease, 2010, 1802(1): 80–91
2. Brown D L, Boden-Albala B, Langa K M, Lisabeth L D, Fair M, Smith M A, Sacco R L, Morgenstern L B. Projected costs of ischemic stroke in the United States. Neurology, 2006, 67(8): 1390–1395
3. Joshi S, Agarwal S. The proposed role of optical sensing in translational stroke research. Annals of the New York Academy of Sciences, 2010, 1199(1): 149–157
4. Li C, Wang L V. Photoacoustic tomography and sensing in biomedicine. Physics in Medicine and Biology, 2009, 54(19): R59–R97
5. Anna Devor S S, Srinivasan V J, Yaseen M A, Nizar K, Saisan P A, Tian P, Dale A M, Vinogradov S A, Maria Angela Franceschini D A B. Frontiers in optical imaging of cerebral blood flow and metabolism. Journal of Cerebral Blood Flow and Metabolism, 2012, 32: 1259– 1276
6. Zhang S, Murphy T H. Imaging the impact of cortical microcirculation on synaptic structure and sensory-evoked hemodynamic responses *in vivo*. PLoS Biology, 2007, 5(5): e119
7. Grant P E, Roche-Labarbe N, Surova A, Themelis G, Selb J, Warren E K, Krishnamoorthy K S, Boas D A, Franceschini M A. Increased cerebral blood volume and oxygen consumption in neonatal brain injury. Journal of Cerebral Blood Flow and Metabolism, 2009, 29 (10): 1704–1713
8. Mesquita R C, Durduran T, Yu G, Buckley E M, Kim M N, Zhou C, Choe R, Sunar U,Yodh A G. Direct measurement of tissue blood flow and metabolism with diffuse optics. Philosophical Transactions of the Royal Society A: Mathematical, Physical and Engineering Sciences, 2011, 369(1955): 4390–4406
9. Obrig H, Steinbrink J. Non-invasive optical imaging of stroke. Philosophical Transactions of the Royal Society A: Mathematical, Physical and Engineering Sciences, 2011, 369(1955): 4470–4494
10. Wilson K, Homan K, Emelianov S. Biomedical photoacoustics beyond thermal expansion using triggered nanodroplet vaporization for contrast-enhanced imaging. Nature Communications, 2012, 3: 618
11. Wang L V. Tutorial on photoacoustic microscopy and computed tomography. IEEE Journal of Selected Topics in Quantum Electronics, 2008, 14(1): 171–179
12. Wang L V. Multiscale photoacoustic microscopy and computed tomography. Nature Photonics, 2009, 3(9): 503–509
13. Wang L V. Prospects of photoacoustic tomography. Medical Physics, 2008, 35(12): 5758–5767
14. Hu S, Gonzales E, Soetikno B, Gong E, Yan P, Maslov K, Lee J M, Wang L V. Optical-resolution photoacoustic microscopy of ischemic stroke. In: Proceedings of SPIE, Photons Plus Ultrasound: Imaging and Sensing. 2011, 7899: 789906
15. Soetikno B, Hu S, Gonzales E, Zhong Q, Maslov K, Lee J M, Wang L V. Vessel segmentation analysis of ischemic stroke images acquired with photoacoustic microscopy. In: Proceedings of SPIE, Photons Plus Ultrasound: Imaging and Sensing. 2012, 8233: 822345
16. Deng Z L, Wang Z, Yang X Q, Luo Q M, Gong H. *In vivo* imaging of hemodynamics and oxygen metabolism in acute focal cerebral ischemic rats with laser speckle imaging and functional photoacoustic microscopy. Journal of Biomedical Optics, 2012, 17(8): 081415
17. Ermilov S A, Khamapirad T, Conjusteau A, Leonard M H, Lacewell R, Mehta K, Miller T, Oraevsky A A. Laser optoacoustic imaging system for detection of breast cancer. Journal of Biomedical Optics, 2009, 14(2): 024007
18. Esenaliev R O, Karabutov A A, Oraevsky A A. Sensitivity of laser opto-acoustic imaging in detection of small deeply embedded tumors. IEEE Journal of Selected Topics in Quantum Electronics, 1999, 5(4): 981–988
19. Ku G, Wang L V. Deeply penetrating photoacoustic tomography in biological tissues enhanced with an optical contrast agent. Optics Letters, 2005, 30(5): 507–509
20. Hamilton J D, O'Donnell M. High frequency ultrasound imaging with optical arrays. IEEE Transactions on Ultrasonics, Ferroelectrics and Frequency Control, 1998, 45(1): 216–235
21. Payne B P, Venugopalan V, Mikić B B, Nishioka N S. Optoacoustic tomography using time-resolved interferometric detection of surface displacement. Journal of Biomedical Optics, 2003, 8(2): 273–280
22. Carp S A, Guerra A, Duque S Q, Venugopalan V. Optoacoustic imaging using interferometric measurement of surface displacement. Applied Physics Letters, 2004, 85(23): 5772–5774
23. Carp S A, Venugopalan V. Optoacoustic imaging based on the interferometric measurement of surface displacement. Journal of Biomedical Optics, 1999, 12(6): 064001
24. Xu Y, Wang L V. Rhesus monkey brain imaging through intact skull with thermoacoustic tomography. IEEE Transactions on Ultrasonics, Ferroelectrics and Frequency Control, 2006, 53(3): 542–548
25. Yang X M, Wang L V. Monkey brain cortex imaging by photoacoustic tomography. Journal of Biomedical Optics, 2008, 13(4): 044009
26. Yao J, Wang L V. Photoacoustic tomography: fundamentals, advances and prospects. Contrast Media & Molecular Imaging, 2011, 6(5): 332–345
27. Dunn A K. Laser speckle contrast imaging of cerebral blood flow. Annals of Biomedical Engineering, 2012, 40(2): 367–377
28. Song L, Elson D S. Effect of signal intensity and camera quantization on laser speckle contrast analysis. Biomedical Optics Express, 2013, 4(1): 89–104
29. He H, Tang Y, Zhou F, Wang J, Luo Q, Li P. Lateral laser speckle contrast analysis combined with line beam scanning illumination to improve the sampling depth of blood flow imaging. Optics Letters, 2012, 37(18): 3774–3776
30. Zhang H Y, Li P, Feng N, Qiu J, Li B, Luo W, Luo Q. Correcting the detrimental effects of nonuniform intensity distribution on fiber-transmitting laser speckle imaging of blood flow. Optics Express, 2012, 20(1): 508–517
31. Song L P, Elson D S. Dual-wavelength endoscopic laser speckle contrast imaging system for indicating tissue blood flow and oxygenation. In: Proceedings of SPIE, Dynamics and Fluctuations in Biomedical Photonics IX. 2012, 8222: 822209
32. Lu H Y, Miao P, Liu Q, Li Y, Tong S B. Dual-modal (OIS/LSCI) imager of cerebral cortex in freely moving animals. In: Proceedings of SPIE, 10th International Conference on Photonics and Imaging in

Biology and Medicine (PIBM 2011). 2012, 8329: 83290P
33. Boas D A, Dunn A K. Laser speckle contrast imaging in biomedical optics. Journal of Biomedical Optics, 2010, 15(1): 011109
34. Parthasarathy A B, Kazmi S M, Dunn A K. Quantitative imaging of ischemic stroke through thinned skull in mice with Multi Exposure Speckle Imaging. Biomedical Optics Express, 2010, 1(1): 246–259
35. Levy H, Ringuette D, Levi O. Rapid monitoring of cerebral ischemia dynamics using laser-based optical imaging of blood oxygenation and flow. Biomedical Optics Express, 2012, 3(4): 777–791
36. Qin J, Shi L, Dziennis S, Reif R, Wang R K. Fast synchronized dual-wavelength laser speckle imaging system for monitoring hemodynamic changes in a stroke mouse model. Optics Letters, 2012, 37 (19): 4005–4007
37. Wang Z, Luo W, Zhou F, Li P, Luo Q. Dynamic change of collateral flow varying with distribution of regional blood flow in acute ischemic rat cortex. Journal of Biomedical Optics, 2012, 17(12): 125001
38. Denk W, Strickler J H, Webb W W. Two-photon laser scanning fluorescence microscopy. Science (New York, NY), 1990, 248 (4951): 73–76
39. Denk W, Svoboda K. Photon upmanship: techreview why multiphoton imaging is more than a gimmick. Neuron, 1997, 18: 351–357
40. Shih A Y, Driscoll J D, Drew P J, Nishimura N, Schaffer C B, Kleinfeld D. Two-photon microscopy as a tool to study blood flow and neurovascular coupling in the rodent brain. Journal of Cerebral Blood Flow and Metabolism, 2012, 32(7): 1277–1309
41. Ginsberg M D, Busto R. Rodent models of cerebral ischemia. Stroke, 1989, 20(12): 1627–1642
42. Kövari E, Gold G, Herrmann F R, Canuto A, Hof P R, Bouras C, Giannakopoulos P. Cortical microinfarcts and demyelination affect cognition in cases at high risk for dementia. Neurology, 2007, 68 (12): 927–931
43. Suter O C, Sunthorn T, Kraftsik R, Straubel J, Darekar P, Khalili K, Miklossy J. Cerebral hypoperfusion generates cortical watershed microinfarcts in Alzheimer disease. Stroke, 2002, 33(8): 1986–1992
44. Hua R, Walz W. The need for animal models in small-vessel brain disease. Critical Reviews in Neurobiology, 2006, 18(1-2): 5–11
45. Mohajerani M H, Aminoltejari K, Murphy T H. Targeted mini-strokes produce changes in interhemispheric sensory signal processing that are indicative of disinhibition within minutes. Proceedings of the National Academy of Sciences of the United States of America, 2011, 108(22): E183–E191
46. Nishimura N, Schaffer C B, Friedman B, Lyden P D, Kleinfeld D. Penetrating arterioles are a bottleneck in the perfusion of neocortex. Proceedings of the National Academy of Sciences of the United States of America, 2007, 104(1): 365–370
47. Nishimura N, Schaffer C B, Friedman B, Tsai P S, Lyden P D, Kleinfeld D. Targeted insult to subsurface cortical blood vessels using ultrashort laser pulses: three models of stroke. Nature Methods, 2006, 3(2): 99–108
48. Schaffer C B, Friedman B, Nishimura N, Schroeder L F, Tsai P S, Ebner F F, Lyden P D, Kleinfeld D. Two-photon imaging of cortical surface microvessels reveals a robust redistribution in blood flow after vascular occlusion. PLoS Biology, 2006, 4(2): e22
49. Watson B D, Dietrich W D, Busto R, Wachtel M S, Ginsberg M D. Induction of reproducible brain infarction by photochemically initiated thrombosis. Annals of Neurology, 1985, 17(5): 497–504
50. Brown C E, Li P, Boyd J D, Delaney K R, Murphy T H. Extensive turnover of dendritic spines and vascular remodeling in cortical tissues recovering from stroke. The Journal of Neuroscience, 2007, 27(15): 4101–4109
51. Mostany R, Portera-Cailliau C. Absence of large-scale dendritic plasticity of layer 5 pyramidal neurons in peri-infarct cortex. The Journal of Neuroscience, 2011, 31(5): 1734–1738
52. Zhang S, Boyd J, Delaney K, Murphy T H. Rapid reversible changes in dendritic spine structure in vivo gated by the degree of ischemia. The Journal of Neuroscience, 2005, 25(22): 5333–5338
53. Drew P J, Shih A Y, Driscoll J D, Knutsen P M, Blinder P, Davalos D, Akassoglou K, Tsai P S, Kleinfeld D. Chronic optical access through a polished and reinforced thinned skull. Nature Methods, 2010, 7(12): 981–984
54. Davalos D, Grutzendler J, Yang G, Kim J V, Zuo Y, Jung S, Littman D R, Dustin M L, Gan W B. ATP mediates rapid microglial response to local brain injury in vivo. Nature Neuroscience, 2005, 8(6): 752–758
55. Sigler A, Murphy T H. In vivo 2-photon imaging of fine structure in the rodent brain: before, during, and after stroke. Stroke, 2010, 41 (10 Suppl): S117–S123
56. Dijkhuizen R M, Ren J M, Mandeville J B, Wu O, Ozdag F M, Moskowitz M A, Rosen B R, Finklestein S P. Functional magnetic resonance imaging of reorganization in rat brain after stroke. Proceedings of the National Academy of Sciences of the United States of America, 2001, 98(22): 12766–12771
57. Li P, Murphy T H. Two-photon imaging during prolonged middle cerebral artery occlusion in mice reveals recovery of dendritic structure after reperfusion. The Journal of Neuroscience, 2008, 28 (46): 11970–11979
58. Murphy T H, Corbett D. Plasticity during stroke recovery: from synapse to behaviour. Nature Reviews. Neuroscience, 2009, 10(12): 861–872
59. Brown C E, Aminoltejari K, Erb H, Winship I R, Murphy T H. In vivo voltage-sensitive dye imaging in adult mice reveals that somatosensory maps lost to stroke are replaced over weeks by new structural and functional circuits with prolonged modes of activation within both the peri-infarct zone and distant sites. The Journal of Neuroscience, 2009, 29(6): 1719–1734
60. Winship I R, Murphy T H. Remapping the somatosensory cortex after stroke: insight from imaging the synapse to network. Neuroscientist, 2009, 15(5): 507–524
61. Carmichael S T. Plasticity of cortical projections after stroke. Neuroscientist, 2003, 9(1): 64–75
62. Carmichael S T. Cellular and molecular mechanisms of neural repair after stroke: making waves. Annals of Neurology, 2006, 59(5): 735–742
63. Coq J O, Xerri C. Acute reorganization of the forepaw representation in the rat SI cortex after focal cortical injury: neuroprotective effects of piracetam treatment. European Journal of Neuroscience, 1999, 11(8): 2597–2608
64. Dancause N, Barbay S, Frost S B, Plautz E J, Chen D, Zoubina E V,

Stowe A M, Nudo R J. Extensive cortical rewiring after brain injury. The Journal of Neuroscience, 2005, 25(44): 10167–10179

65. Nudo R J, Milliken G W. Reorganization of movement representations in primary motor cortex following focal ischemic infarcts in adult squirrel monkeys. Journal of Neurophysiology, 1996, 75(5): 2144–2149
66. Rouiller E M, Yu X H, Moret V, Tempini A, Wiesendanger M, Liang F. Dexterity in adult monkeys following early lesion of the motor cortical hand area: the role of cortex adjacent to the lesion. European Journal of Neuroscience, 1998, 10(2): 729–740
67. Castro-Alamancos M A, Borrel J. Functional recovery of forelimb response capacity after forelimb primary motor cortex damage in the rat is due to the reorganization of adjacent areas of cortex. Neuroscience, 1995, 68(3): 793–805
68. Dijkhuizen R M, Singhal A B, Mandeville J B, Wu O, Halpern E F, Finklestein S P, Rosen B R, Lo E H. Correlation between brain reorganization, ischemic damage, and neurologic status after transient focal cerebral ischemia in rats: a functional magnetic resonance imaging study. The Journal of Neuroscience, 2003, 23(2): 510–517
69. Rossini P M, Altamura C, Ferreri F, Melgari J M, Tecchio F, Tombini M, Pasqualetti P, Vernieri F. Neuroimaging experimental studies on brain plasticity in recovery from stroke. Europa Medicophysica, 2007, 43(2): 241–254
70. Schaechter J D, Moore C I, Connell B D, Rosen B R, Dijkhuizen R M. Structural and functional plasticity in the somatosensory cortex of chronic stroke patients. Brain, 2006, 129(10): 2722–2733
71. Johnston D G, Denizet M, Mostany R, Portera-Cailliau C. Chronic in vivo imaging shows no evidence of dendritic plasticity or functional remapping in the contralesional cortex after stroke. Cerebral Cortex, 2012,
72. Kleinfeld D, Mitra P P, Helmchen F, Denk W. Fluctuations and stimulus-induced changes in blood flow observed in individual capillaries in layers 2 through 4 of rat neocortex. Proceedings of the National Academy of Sciences of the United States of America, 1998, 95(26): 15741–15746
73. Devor A, Tian P, Nishimura N, Teng I C, Hillman E M C, Narayanan S N, Ulbert I, Boas D A, Kleinfeld D, Dale A M. Suppressed neuronal activity and concurrent arteriolar vasoconstriction may explain negative blood oxygenation level-dependent signal. The Journal of Neuroscience, 2007, 27(16): 4452–4459
74. Tian P, Teng I C, May L D, Kurz R, Lu K, Scadeng M, Hillman E M C, De Crespigny A J, D'Arceuil H E, Mandeville J B, Marota J J, Rosen B R, Liu T T, Boas D A, Buxton R B, Dale A M, Devor A. Cortical depth-specific microvascular dilation underlies laminar differences in blood oxygenation level-dependent functional MRI signal. Proceedings of the National Academy of Sciences of the United States of America, 2010, 107(34): 15246–15251
75. Kobat D, Durst M E, Nishimura N, Wong A W, Schaffer C B, Xu C. Deep tissue multiphoton microscopy using longer wavelength excitation. Optics Express, 2009, 17(16): 13354–13364
76. Kirchhoff F, Debarbieux F, Kronland-martinet C, Cojocaru G, Popa-Wagner A. Combined two-photon laser-scanning microscopy and spectral microCT X-ray imaging to characterize the cellular signature and evolution of microstroke foci. Romanian Journal of Morphology and Embryology, 2012, 53(3 Suppl): 671–675
77. Feng G, Mellor R H, Bernstein M, Keller-Peck C, Nguyen Q T, Wallace M, Nerbonne J M, Lichtman J W, Sanes J R. Imaging neuronal subsets in transgenic mice expressing multiple spectral variants of GFP. Neuron, 2000, 28(1): 41–51
78. Helmchen F, Fee M S, Tank D W, Denk W. A miniature head-mounted two-photon microscope. high-resolution brain imaging in freely moving animals. Neuron, 2001, 31(6): 903–912
79. Piyawattanametha W, Cocker E D, Burns L D, Barretto R P J, Jung J C, Ra H, Solgaard O, Schnitzer M J. *In vivo* brain imaging using a portable 2.9 g two-photon microscope based on a microelectromechanical systems scanning mirror. Optics Letters, 2009, 34(15): 2309–2311
80. Risher W C, Ard D, Yuan J, Kirov S A. Recurrent spontaneous spreading depolarizations facilitate acute dendritic injury in the ischemic penumbra. The Journal of Neuroscience, 2010, 30(29): 9859–9868